SPATIAL ANALYSIS OF TURBULENT FLOW FIELS BY DETERMINISTIC AND STOCHASTIC APPROACHES

B. Crippa, L. Mussio
Politecnico di Milano
Dipartimento I.I.A.R. - Sezione di Rilevamento
Piazza Leonardo da Vinci, 32
20133 Milano
ITALY

H.G. Maas
Institute of Geodesy and Photogrammetry
Swiss Federal Institute of Technology
ETH - Hoenggerberg
CH -8093 Zurich

ABSTRACT:
Objects transparent to wavelenghts to which photogrammetric sensors are sensitive or opaque objects with fractal dimension near to three are 3D (real) examples in photogrammetric practice. The spatial analysis of 3D objects involves deterministic and stochasticapproaches. The former concerns the finite element method by using spline interpolation, the latter implies an optimal filtering of a signal from noise by covariance estimation, covariance function modelling and collocation. An application shows the discussed spatial analysis methods to velocity fields in turbulent flows determined by 3D particle tracking velocimetry.

KEY WORDS: 3D, Algorithm, Accuracy

1. THE PROBLEM

Three - dimensional particle tracking velocimetry (3D-PTV) is a well known technique for the determination of three-dimensional velocity fields in flows. It is based on the discrete visualization of flows with small, reflecting, neutrally buoyand tracer particles and a stereoscopic recording of image sequences of the particles marking the flow. A powerful 3D PTV has been developed at the Swiss Federal Institute of Technology in a cooperation of the Institute of Geodesy and Photogrammetry with the Institute of Hydromechanics and Water Resources Management (Papantoniou/Dracos, 1989; Papantoniou/Maas, 1990; Maas, 1990, 1992). A flow scheme of this 3D-PTV is shown in Figure 1.1.

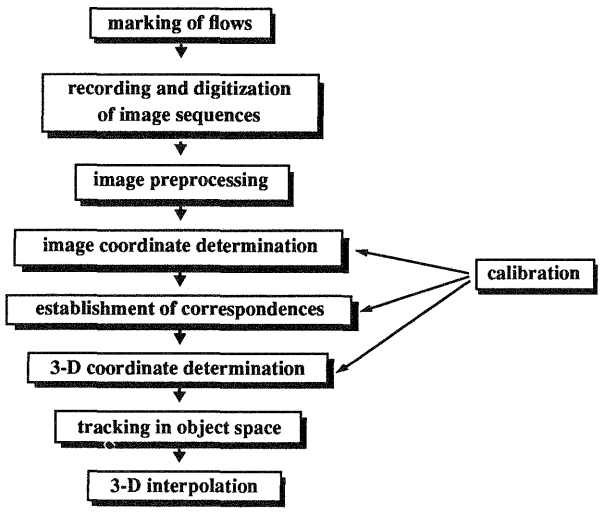

Figure 1.1 - Flow scheme of a 3D-PTV

There are two different goals in the application of PTV: one is to follow a relatively small number of particles over a longer period of time in order to do Lagrangian statistics on the particles trajectories, the other is the determination of instantaneous velocity fields from a large number of particles. Due to the highseeding density required by this second goal some ambiguity problems occur in the identification of particle images, in the establishment of stereoscopic correspondence (Maas, 1992b) and in tracking (Malik et al., 1992). It can be shown that with a simple stereoscopic camera arrangement positions of at maximum 300-400 particles can be determined reliably. Systems for higher spatial resolutions have to be based on three or even four cameras imaging the flow synchronously in order to be able to solve ambiguities in the establishment of stereoscopic correspondences (Maas, 1992b).
Using standard video hardware equipment (CCIR norm cameras, images digitized to 512x512 pixels) a maximum of 1000 simultaneous velocity vectors at a temporal resolution of 25 velocity fields per second could be determined in practical experiments. The standard deviation of particle coordinates in an observation volume of about 200x160x50 mm^3 determined by a three-camera system was 0.06 mm in X,Y and 0.18 mm in Z (depth coordinate). Due to imperfections of the calibration, illumination effects and influences of the shape and surface properties of particles their coordinates in consecutive datasets are correlated; it could be proved that the accuracy of the displacement vectors derived from the particle coordinates is significantly better than the standard deviation of particle coordinates (Papantoniou-Maas, 1990).
The result of a 3D-PTV is a set of velocity vectors at random positions in a 3D observation volume which has to be interpolated onto a regular grid. Figure 1.2 and Figure 1.3 show two examples of measured velocity fields.

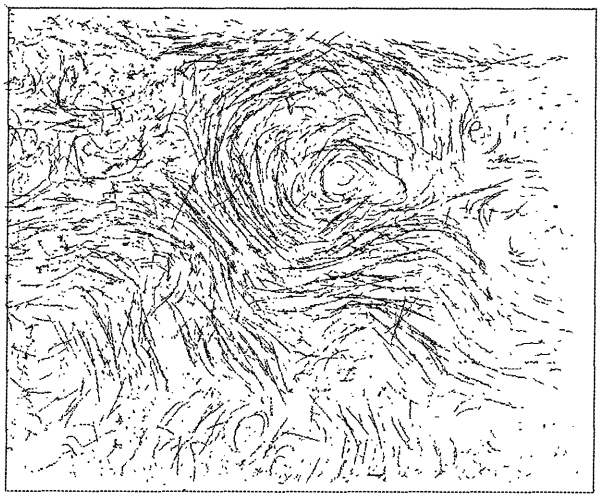

Figure 1.2- PTV - Example 1: velocity field in a turbulent channel flow (1 second of flow data with about 500 simultaneous velocity vectors, 2D-projection)

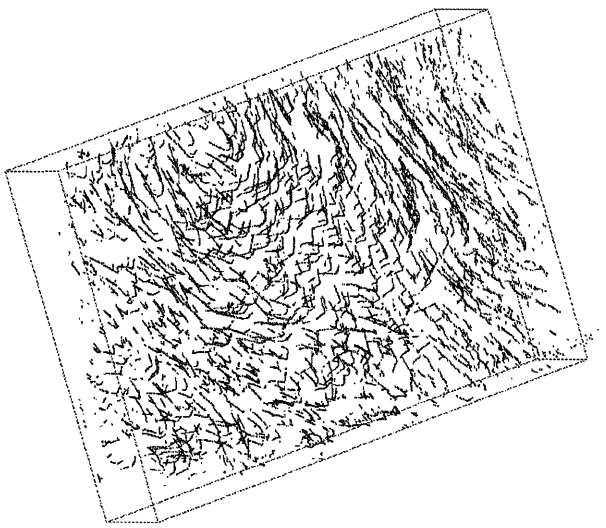

Figure 1.3- PTV - Example 2: velocity field generated in a aquarium (0.5 seconds of flow data with about 800 simultaneous velocity vectors, 2D-projection)

Another example of 3D data acquisition is the application of 3D laser induced fluorescence (3D-LIF) to examinations of mixing processes (Dahm et al., 1990). Unlike PTV, LIF is based on continuous visualization of flow structures by fluorescent material, which emits light of a certain wavelength l_2 when animated by a laser with a different wavelength l_1. By scanning an observation volume with a laser lightsheet in depth and recording images of the illuminated slices with high-speed cameras, 3D fluorescence concentration data can be acquires quasi-simultaneously. From these data e.g. concentration gradient vector fields and scalar energy dissipation fields can be derived, which contain information about the efficiency of mixing processes.

2. THE METHOD

(This paragraph contains an exposition of the deterministic and stochastic approaches, with special regard to 3D problems; for a view over 2D problems and time series and for more information see: Sansò/Tcherning, 1983; Ammanati et al., 1983; Sansò/Schuh, 1987; de Haan/Mussio, 1989; Barzaghi/ Crippa, 1990).

2.1 Covariance estimation and covariance function modelling

The collocation method requires appropriate models to interpolate the empirical autocovariance and crosscovariance function of the signal, obtained from the residuals of linear interpolations.
This model function is used (in addition to the model found by linear interpolation) to predict the value of the studied quantities.
An hypothesis was made: the residuals can be seen as realizations of a continuous, isotropic, and normal stochastic process which is stationary of 2nd order with mean zero and covariance function of the kind:

$$C(P_1,P_2) = C(\|P_1 - P_2\|)$$

With $X(P_i)$ the n observations at the different points $P_1,\dots,P_i,\dots,P_n$ the estimate of the empirical autocovariance function at the space interval $r^{(1)}$ is calculated from:

$$\gamma\left[r^{(1)}\right] = \frac{1}{n} \sum_{i=1}^{n} v_i \frac{1}{n_i^{(1)}} \sum_{j=1}^{n_i^{(1)}} v_j^{(1)}$$

$$\text{where } \left\{v_j^{(1)}: \forall P_j \Rightarrow r^{(1-1)} < \|P_i - P_j\| \le r^{(1)}\right\}$$

$$\text{and} \quad v_k = x_k - \bar{x} \quad k = 1,n$$

and the estimates of empirical crosscovariance function at the space interval $r^{(1)}$ are computed from:

$$\gamma_{xy}\left[r^{(1)}\right] = \frac{1}{n+m}\left[\sum_{i=1}^{n} v_i \frac{1}{n_i^{(1)}} \sum_{j=1}^{m_i^{(1)}} w_j^{(1)} + \sum_{i=1}^{m} w_i \frac{1}{m_i^{(1)}} \sum_{j=1}^{n_i^{(1)}} v_j^{(1)}\right]$$

$$\text{where } \left\{v_j^{(1)}: \forall P_j \Rightarrow r^{(1-1)} < \|P_i - P_j\| \le r^{(1)}\right\}$$

$$\left\{w_j^{(1)}: \forall P_j \Rightarrow r^{(1-1)} < \|P_i - P_j\| \le r^{(1)}\right\}$$

and $v_k = x_k - \bar{x} \quad k = 1,n$

$w_k = y_k - \bar{y} \quad k = 1,m$

A criterion for the choice of the radius of the sphere including the first autocovariance zone is maximizing the first autocovariance estimate as follows:

$$r^{(1)}: \gamma\left[r^{(1)}\right] = \max\left[\gamma\left[r^{(1)}\right]\right]$$

$$\text{where } \gamma\left[r^{(1)}\right] = \frac{1}{n}\sum_{i=1}^{n} v_i \frac{1}{n_i^{(1)}} \sum_{j=1}^{n_i^{(1)}} v_j^{(1)}$$

$$\text{and } \left\{v_j^{(1)}: \forall P_j \Rightarrow 0 < \| P_i - P_j \| \le r^{(1)}\right\}$$

The "best fit" of the autocovariance function of the signal is then chosen among some available models, namely:

E $\gamma(r) = a \exp(-br)$

N $\gamma(r) = a \exp(-br^2)$

EP $\gamma(r) = a \exp(-br)\ (1-cr^2)$

NP $\gamma(r) = a \exp(-br^2)\ (1-cr^2)$

ES $\gamma(r) = a \exp(-br)\ \sin(cr)/(cr)$

NS $\gamma(r) = a \exp(-br^2)\ \sin(cr)/(cr)$

EJ $\gamma(r) = 2a \exp(-br)\ J_1(cr)/(cr)$

NJ $\gamma(r) = 2a \exp(-br^2)\ J_1(cr)/(cr)$

where the smoothness given by the coefficient b for the cases EP and NP is very high. The previous abbreviations indicate respectively:

E exponential function;

N normal function;

P parabole function;

S sine function over x;

J Bessel function of 1st order over x.

This list has been built according to the definition of covariance function: positive power, i.e. positive 3D Fourier transform, and Schwarz condition for vectorial processes. New covariance function can be created from old by applying following fundamental theorems:

- a linear combination with positive coefficients;
- a product;
- a convolution.

The same list is used to interpolate crosscovariance functions: it is not correct in principle, but is acceptable in practice, provided that crosscovariance estimates are low enough.
Besides, since 3D isotropic finite covariance functions are not known, a 3D finite covariance function, isotropic from the numerical point of view, can be found using a tricubic spline function:

$$\gamma(r) \cong S(x,y,z) = S(x)\ S(y)\ S(z)$$

Finally, the noise variance is found as:

$$\sigma_n^2 = \sigma^2 - \sigma_s^2 = \sigma^2 - a$$

and the noise covariance can be found with a similar formula.

2.2 Filtering, prediction and crossvalidation

By using an hybrid norm:

$$\phi = \hat{s}^t C_{ss}^{-1} \hat{s} + \hat{n}^t \hat{n} / \sigma_n^2 + \lambda^t(\hat{s} + \hat{n} - v^\circ) = \min$$

the residuals v° can be split in two parts: the signal s and the noise n:

$$\hat{s} = C_{ss} C_{vv}^{-1} v^\circ = v^\circ - \hat{n}$$

$$\hat{n} = v^\circ - \hat{s} = \sigma_n^2 C_{vv}^{-1} v^\circ$$

$$\text{where } C_{vv} = C_{ss} + \sigma_n^2 I$$

and $C_{ss} = [\gamma(r)]$ is the matrix of autocovariance of the signal, I is the unitary matrix of the same dimension as C_{ss}.
As regard the accuracy, the variance-covariance matrix of the error of the estimated signal is given by:

$$C_{ee} = C_{ss} - C_{ss} C_{vv}^{-1} C_{ss} = \sigma_n^2 I - \sigma_n^4 C_{vv}^{-1} =$$

$$= \sigma_n^2 I - C_{\hat{n}\hat{n}}$$

i.e. for the main diagonal elements:

$$\sigma_e^2 = \sigma_s^2 - c_{ss}^t C_{vv} c_{ss} = \sigma_n^2 - \sigma_n^4 \operatorname{diag}(C_{vv}^{-1})$$

where $e = s - \hat{s}$

and $C_{\hat{n}\hat{n}} = \sigma_n^4 C_{vv}^{-1}$

while a posteriori an estimate of variance of the noise is supplied by:

$$\hat{\sigma}_n^2 = \hat{n}^t \hat{n} / \operatorname{Tr}\left[\sigma_n^2 C_{vv}^{-1}\right]$$

The same relationships are employed for the prediction of the signal s in points where no observations are generally available:

$$\hat{s}_p = c^t_{ss_p} C^{-1}_{vv} v^\circ = c^t_{ss_p} y \qquad ; \qquad y = C^{-1}_{vv} v^\circ$$

$$\sigma^2_{e_p} = \sigma^2_{s_p} - c^t_{ss_p} C^{-1}_{vv} c_{ss_p}$$

where $e_p = s_p - \hat{s}_p$

At the check points, if any, discrepances can be computed by:

$$\hat{\delta} = w^\circ_p - \hat{s}_p$$

where w°_p are a small set of data use for the crossvalidation.

2.3 Finite element method (e.g. tricubic spline interpolation)

A tricubic spline function is given by the product of three orthogonal cubic spline functions:

$$S(x,y,z) = S(x)\ S(y)\ S(z)$$

The choice for the number of cells and the number of knots depends on the number of observations m and the interpolation step δ.
The number of cells is the product of the number of classes in three directions x,y and z:

$$\nu = \nu_x\ \nu_y\ \nu_z$$

where $\nu_x = \text{int}\ (\Delta X/\delta) + 1$
$\nu_y = \text{int}\ (\Delta Y/\delta) + 1$
$\nu_z = \text{int}\ (\Delta Z/\delta) + 1$

being ΔX, ΔY and ΔZ the dimensions of the space region in three directions and δ the chosen interpolation step. Consequently the number of knots is:

$$n = n_x\ n_y\ n_z = (\nu_x + 3)\ (\nu_y + 3)\ (\nu_z + 3)$$

The tricubic spline interpolation is performed, as a classical least squares problem, by writing a system of observation equations:

$$\hat{s}_k = s^\circ_k + \hat{v}_k = \qquad k = 1,m$$

$$= \sum_{i=1}^{4}\sum_{j=1}^{4}\sum_{l=1}^{4} \hat{a}_{I+i\ J+j\ L+l}\ S_{ijl}(\xi_k, \eta_k, \zeta_k)$$

and associating it with the least squares norm:

$$\phi = \sum_{k=1}^{m} \hat{v}^2_k = \min$$

The weights are mostly assumed equal one; however more complex stochastic model should be defined including correlations between the observations, but they are usually omitted in sake of brevity.
The following formulas are the legenda of the functional model; indeed for the x direction, the coordinate of the k-th knot respect the initial corner is splitted in two parts:

$$\Delta x_k = I\ \delta + \delta x_k$$

where the number of the preceding knots is:

$$I = \text{int}\ (\Delta x_k/\delta)$$

and the position inside the class is:

$$\xi_k = \delta x_k/\delta$$

being $\delta x_k = \Delta x_k - I\delta$

analogously, for the y direction:

$$\Delta y_k = J\ \delta + \delta y_k$$

where $J = \text{int}\ (\Delta y_k/\delta)$

and $\eta_k = \delta y_k/\delta$

being $\delta y_k = \Delta y_k - I\delta$

and for the z direction:

$$\Delta z_k = L\ \delta + \delta z_k$$

where $L = \text{int}\ (\Delta z_k/\delta)$

and $\zeta_k = \delta z_k/\delta$

being $\delta z_k = \Delta z_k - I\delta$

Note that suitable constraints for the knots should be introduced at the border and in empty regions.

3. THE SYSTEM OF PROGRAMS

(Because of the modularity of the system of programs, there is a high degree of similarity between this system and those dedicated to 2D problems and time series; see: Crippa/Mussio, 1987.)

The system consists of a set of programs, which allow for the following operations:

1) data management;

2) simple least squares interpolation, to remove the non-stationary trend;

3) search for the optimum spacing, for the computation of empirical values of the covariance functions, when the date are not regularly gridded;

4) empirical estimation of the autocovariance and crosscovariance functions of stochastic processes with some average invariance property with respect to a suitable group of coordinate transformations;

   (steps 2, 3 and 4 are repeated until the empirical covariance functions look as non-stationary covariance);

5) interpolation of empirical functions by means of suitable positive definited models, especially with finite covarince function;

6) finite elements interpolation, by tricubic splines, to solve some computational problems, if any, and save computing time;

   (steps 3, 4, 5 and 6 are repeated until computational problems remain in filtering);

7) filtering of the noise from the signal and computation of the m.s.e. of the estimated signal;

8) analysis of the noise by means of data snooping of Baarda type;

   (by using the residual noise, steps 4 and 5 are newly executed; if its empirical covariance functions look as coloured residual noise, a new step of collocation is started);

9) prediction of the signal on check points and/or on the points of a regular grid;

10) plot of results by suitable graphics representation.

Figure 3.1 shows the flow chart of the system of programs.
When estimating the covariance function of a process in three dimensions on a large set of data, particular care must be taken of the numerical procedure used, to avoid wasting of computing time. To this aim special algorithms of sorting, merging and clustering have been implemented in order to obtain quick identification of neighboring points. The same care is required for the data management.
It is at this level that a first blunder rejection is done: this is achieved simply by comparing each point value with a moving average taken on the neighboring points only. This is considered as a pure blunder elimination, while the more refined analysis described at step 8 is used to recognize particular features of the model.
Indeed, if the data are regularly gridded, the analysis of the characteristics of the noise and its slope and bending allows for the discrimination between outliers and break lines. The same is true, with minor changes, when the data are not regularly gridded but their density is generally high. Finally, if the density is low, no information on the break lines is available as output data.

When filtering the noise from the signal of a process in three dimensions on large set of data, particular care should be taken of the numerical procedure to avoid wasting of computing time: to this aim the conjugate gradient method (with preconditioning and reordering algorithms, if necessary) is used.
As regard the vectorial processes, all the components are filtered simultaneously, when the crosscorrelations are not too high. Otherwise, because of the ill-conditioned system, the components must be filtered separately, to avoid numerical problem.
After the filtering the residual crosscorrelations should be considered in a second step, if neccessary.

4. THE TEST EXAMPLES

The system of programs runs on the SUN Spark and DIGITAL Vax computers.
Two real examples of turbolence flow fields are used to test the new system.
The study of these examples has been completed for small sets of data and it will be repeated in the future considering all data together.
The first example contains 811 observations, which are irregularly distributed but dense (average distance among neighboring going to equal to 10 μm); the second one contains 452 observations with the same kind of distribution (average distance among neighboring points equal to 5 μm).
Their behaviour is very rough. Indeed the residuals, after a polynomial interpolation of the second order, have approximately the same size and shape. This means that the trend removal should not be very important in this case.
However, when, the correlation length is quite large, the filtering by least squares collocation will give serious computation problems when the set of data is large. For this reason a pre-filtering must be done. The easiest way to perform this seems to be the finite elements method. The same technique has been indipendently applied for a suboptimal filtering from a statistical point of view, but with reduced computing time and memory requirements. Besides the solution is well-conditioned, from a numerical point of view.
Therefore the "old" residuals have been interpolated by bicubic spline functions (their lags are 50 and 25 μm in the first example and 50, 25 and 15 μm in the second one) and "new" residuals have been obtained. This operation will furnish a correlation length of reasonable size.
At the moment because the sets of data are small, the filtering by least squares collocation has been directly performed without computational problems. The residual noise of the both examples is very flat, and their covariance functions look as those of white noise processes. Note that a filtering by stochastic approach is preferable with respect to expanding the finite elements model by reducing the lag of the bicubic spline functions. Indeed the capability to follow the fields behaviour is in the first case higher than in the second one.
Table 4.1 summarizes the results obtained by processing the two examples.
The evaluation of the results has not yet been done by the expert of hydromechanics; nevertheless the values of the a posteriori variance of the noise and the estimation error corfirm the values of the standard deviation of the observations for the

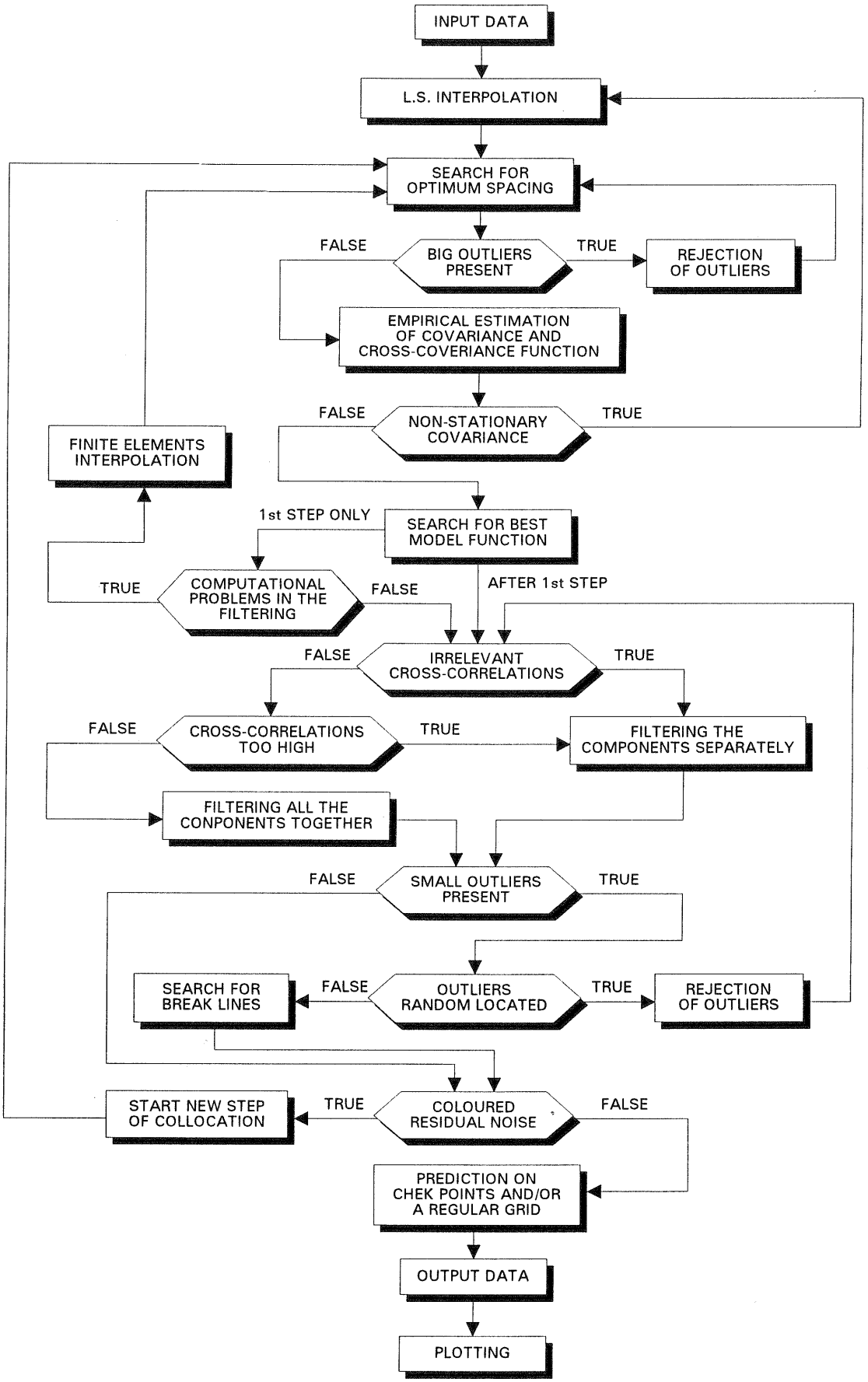

Figure 3.1- Flow chart of the system of programs

first example. The second example gives worse results, since there are less points and the turbolence is higher.

Table 4.1- Spatial analysis of turbolent flow fields (unit: mm)

	1st example (n = 811)			2nd example (n = 452)		
	x	y	z	x	y	z
- a priori standard deviation:	.315	.206	.286	.218	.348	.348
- 2nd order polynomial interpolation:						
a posteriori sigma naught	.205	.145	.259	.205	.208	.344
- covariance functions:	(NS)	(ES)	(ES)	(NS)	(NS)	(ES)
(insignificant crosscovariances)						
a priori variance of the signal	.144	.106	.142	.156	.148	.149
a priori variance of the noise	.120	.084	.174	.104	.120	.246
best correlation coefficient	58%	54%	28%	68%	58%	24%
optimal radius	10	10	10	5	5	5
correlation length	30	20	10	20	15	10
"zero point"	100	100	100	50	50	50
number of blunders (α = 1%)	26	26	20	12	15	15
- collocation filtering:						
a posteriori variance of the signal	.145	.091	.087	.164	.154	.124
a posteriori variance of the noise	.114	.076	.183	.094	.115	.266
estimation error	.066	.060	.112	.079	.086	.125
number of outliers (α = 5%)	38	36	33	25	34	41
trimmed variance of the noise	.094	.064	.148	.073	.092	.185
- finite element method by using tricubic splines:						
interpolation step	50	25		50	25	15
number of knots	44	192		24	60	132
a posteriori sigma naught x	.152	.123		.177	.153	.128
y	.133	.109		.189	.160	.133
z	.253	.224		.336	.326	.316

APPENDIX

Least squares collocation with stochastic - and non-stochastic parameters

(This appendix presents a development of basic ideas of Barzaghi et al., 1988; and is quoted with minor changes from Crippa/de Haan/Mussio, 1989).

In the above mentioned procedure different systems are solved successively. In the integrated geodesy approach all systems are solved simultaneously. Thus after the linearization of the observation and pseudo-observation equations, the observables and the other data α are collected in a unique system containing uncorrelated unknowns x as well as correlated unknowns that can be interpreted as stochastic signal s to filter from the random noise n:

$$\alpha = Ax + Bs$$

Note that it is necessary to perform preceding separate adjustments. Indeed the covariance matrix of the signal C_{ss} is obtained from estimates for the unknown parameters or residuals; moreover the variance of the noise σ_n^2 is assumed equal to the sigma naught square obtained in the last preceding separate adjustment.
The use of both stochastic and non-stochastic parameters causes the need to introduce a hybrid norm:

$$\frac{1}{2}[\hat{s}^t \; \hat{n}^t] \begin{bmatrix} C_{ss}^{-1} & 0 \\ 0 & P/\sigma_n^2 \end{bmatrix} \begin{bmatrix} \hat{s} \\ \hat{n} \end{bmatrix} + \lambda^t(A\hat{x} + B\hat{s} - \hat{n} - \alpha^\circ) = \min$$

where α° indicates the observations, $\hat{x}$, $\hat{s}$ and $\hat{n}$ the estimated values of x, s and n respectively, P the weight matrix of the observations and λ a vector of Lagrange multipliers.

This can give some trouble in the fixing of the weights of the different elements. However by repeating the integrated geodesy approach adjustment, the uncertainty about the weight ratios can be eliminated, and suitable values for the weights can be established.
Moreover all the data are supposed outlier free; however because outliers occur in the data, due to gross errors and/or unmodelled effects, a suitable strategy combining robustness and efficiency has to be used. Indeed robust estimators are useful for the identification of suspected outliers, while the least squares are very powerful for testing about acceptance or rejection.
The system of observation equations is now rewritten as:

$$\alpha = Bs$$

with s containing both stochastic and non-stochastic parameters $s^t=[x^t s^t]$ and the design matrix B defined as B = [A B], expressing both the chosen functional and stochastic modelling. The observations α° are related to the estimates $\hat{s}$ of s by the same linearized model:

$$B\hat{s} - \hat{n} - \alpha^\circ = 0 \qquad (A.1)$$

The covariance matrix C_{ss} for the newly defined signal s contains four blocks, two diagonal blocks containing the covariance matrices of the stochastic and non-stochastic part of the signal, and two zero off-diagonal blocks:

$$C_{ss} = \begin{bmatrix} hI & 0 \\ 0 & C_{ss} \end{bmatrix}$$

The covariance matrix of the stochastic parameters is determined by one or more auto and crosscovariance functions, which can be estimated empirically with the results of preceding separate adjustments. The covariance matrix of the non stochastic parameters is a diagonal matrix, the elements of which have to be chosen in balance with the variances of the stochastic parameters: in such a way that the solution is not contrained too much to either type of parameters. The general variance of the noise σ_n^2, which also has to be known a priori, can be assumed equal to the estimated variance factor σ_o^2 of the last separate preceding adjustment.
The least squares criterion can now be used to minimize contemporaneously the norm $\hat{s}^t C_{ss}^{-1} \hat{s}$ and the norm of the residuals of the observation equations $\hat{n}^t P \hat{n}/\sigma_n^2$:

$$\frac{1}{2}[\hat{s}^t \; \hat{n}^t] \begin{bmatrix} C_{ss}^{-1} & 0 \\ 0 & P/\sigma_n^2 \end{bmatrix} \begin{bmatrix} \hat{s} \\ \hat{n} \end{bmatrix} + \lambda^t(B\hat{s} - \hat{n} - \alpha^\circ) = \min$$

with P the weight matrix of the observations and λ a vector of Lagrange multipliers. According to this criterion, the estimates for the signal and the noise become (taking into account expression 1.1):

$$\hat{s} = C_{ss} B^t (BC_{ss} B^t + \sigma_n^2 P^{-1})^{-1} \alpha^\circ \qquad (A.2)$$

$$\hat{n} = \sigma_n^2 P^{-1} (BC_{ss} B^t + \sigma_n^2 P^{-1})^{-1} \alpha^\circ = \alpha^\circ - B\hat{s} \qquad (A.3)$$

The computation of expressions (A.2) and (A.3) requires the solution of a system with dimension m, equal to the number of observations. It would however be more convenient to have analogous expressions, which require the solution of a system with dimension n < m, equal to the number of parameters. A further requirement would be the absence of inverse matrices which contain inverse matrices. Both can be achieved by the application of the two theorems of linear algebra, which are stated below:

$$(Q \pm RST)^{-1} = Q^{-1} \mp Q^{-1}R\,(S^{-1} \pm TQ^{-1}R)^{-1}TQ^{-1} \qquad (A.4)$$

$$Q^{-1}(Q^{-1} \pm S)^{-1}Q^{-1} = (Q \pm QSQ)^{-1} \qquad (A.5)$$

Precisely, applying first two times theorem (A.4) and then theorem (A.5), one obtains:

$$(BC_{ss} B^t + \sigma_n^2 P^{-1})^{-1} =$$

$$+ P/\sigma_n^2 - PB\,(\sigma_n^2 C_{ss}^{-1} + B^tPB)^{-1}B^tP/\sigma_n^2 =$$

$$= P/\sigma_n^2 - PB\,(B^tPB)^{-1}B^tP/\sigma_n^2 +$$

$$+ PB(B^tPB)^{-1}[C_{ss} + \sigma_n^2(B^tPB)^{-1}]^{-1}(B^tPB)^{-1}B^tP =$$

$$= P/\sigma_n^2 - PB(B^tPB)^{-1}B^tP/\sigma_n^2 +$$

$$+ PB(B^tPBC_{ss}B^tPB + \sigma_n^2 B^tPB)^{-1}B^tP$$

The estimate for the noise can now be rewritten as:

$$\hat{n} = \alpha^\circ - B[(B^tPB)^{-1} - \sigma_n^2(B^tPBC_{ss}B^tPB + \sigma_n^2B^tPB)^{-1}]B^tP\alpha^\circ$$

$$= \alpha^\circ - Bs \qquad (A.6)$$

Taking into account expression (A.6) the estimate for the signal becomes:

$$\hat{s} = (B^tPB)^{-1}B^tP\alpha^\circ +$$

$$- \sigma_n^2\,(B^tPBC_{ss}B^tPB + \sigma_n^2\,B^tPB)^{-1}B^tP\alpha^\circ \qquad (A.7)$$

With these new expressions, the law of variance propagation permits the expression of the corresponding covariance matrices in equally convenient forms. The covariance matrix of the estimated signal and the residual noise become respectively:

$$C_{\hat{s}\hat{s}} = C_{ss} - \sigma_n^2 (B^t P B)^{-1} + \\ + \sigma_n^4 (B^t P B C_{ss} B^t P B + \sigma_n^2 B^t P B)^{-1} \quad (A.8)$$

$$C_{\hat{n}\hat{n}} = \sigma_n^2 [P^{-1} - B(B^t P B)^{-1} B^t] + \\ + \sigma_n^4 B(B^t P B C_{ss} B^t P B + \sigma_n^4 B^t P B)^{-1} B^t \quad (A.9)$$

Moreover, taking into account (A.1), the estimated value of the observables can be written as:

$$\hat{\alpha} = \alpha^\circ - \hat{n} = B\hat{s} \quad (A.10)$$

Applying the law of variance propagation, its covariance matrix becomes:

$$C_{\hat{\alpha}\hat{\alpha}} = B C_{\hat{s}\hat{s}} B^t \quad (A.11)$$

Finally, indicating with the symbol e the error in the estimate of the signal, i.e. the difference between its theoretic value and its estimate: $e = s - \hat{s}$, the covariance matrix C_{ee} becomes, taking into account (A.8), and applying the law of covariance propagation,

$$C_{ee} = C_{ss} - C_{\hat{s}\hat{s}} = \\ \sigma_n^2 (B^t P B)^{-1} + \sigma_n^4 (B^t P B C_{ss} B^t P B + \sigma_n^2 B^t P B)^{-1} \quad (A.12)$$

Consequently one has:

$$C_{\hat{s}\hat{s}} = C_{ss} - C_{ee} \quad (A.13)$$

and:

$$C_{\hat{n}\hat{n}} = \sigma_n^2 P^{-1} - B C_{ee} B^t = \sigma_n^2 P^{-1} - C_{\varepsilon\varepsilon} \quad (A.14)$$

where the last matrix in expression (A.14) is the covariance matrix of the estimate for the expected value of the observables:

$$C_{\varepsilon\varepsilon} = B C_{ee} B^t \quad (A.15)$$

having indicated with ε the error of the estimate of the expected value of the observables, i.e. the difference between its theoretical value and its estimate:

$$\varepsilon = \alpha - \hat{\alpha} = B(s - \hat{s}) = Be$$

The least squares criterion, expressed in the formulation of the collocation method, can provide, besides an estimate for a filtered signal, also an estimate for a predicted signal $s_p = t$: the stochastic parameters can also be estimated in every point. One has to keep in mind however, that only the properly called stochastic parameters can be estimated.
Consequently the covariance matrix C_{tt} only consists of the properly called stochastic parameters, and the crosscovariance matrix between the filtered and the predicted signal C_{st} ($C_{st} = C_{st}^t$) is divided in two parts: one containing the covariance between the predicted signal and the properly called stochastic parameters in the filtered signal, and one identically zero. This null matrix is exactly the reason of the impossibility to predict the parameters, which are strictly non stochastic.
Given the functional:

$$\frac{1}{2} [\hat{s}^t \; \hat{t}^t \; \hat{n}^t] \begin{bmatrix} \begin{bmatrix} C_{ss} & C_{st} \\ C_{ts} & C_{tt} \end{bmatrix}^{-1} & 0 \\ 0 \quad 0 & P/n \end{bmatrix} \begin{bmatrix} \hat{s} \\ \hat{t} \\ \hat{n} \end{bmatrix} + \\ + \lambda (B\hat{s} - 0\hat{t} + \hat{n} - \alpha^\circ) = \min$$

λ being a vector of Lagrange multipliers, and taking into account expression (A.7), one has:

$$\hat{t} = C_{ts} B^t (B C_{ss} B^t + \sigma_n^2 P^{-1})^{-1} \alpha^\circ = \\ = C_{ts} B^t P B (B^t P B C_{ss} B^t P B + \sigma_n^2 B^t P B)^{-1} B^t P \alpha^\circ \quad (A.16)$$

or:

$$\hat{t} = C_{ts} z$$

with z a service vector:

$$z = B^t P B (B^t P B C_{ss} B^t P B + \sigma_n^2 B^t P B)^{-1} B^t P \alpha^\circ$$

which is to be computed once at the end of the filtering.
Applying the law of covariance propagation, the covariance matrix of the predicted signal becomes:

$$C_{\hat{t}\hat{t}} = C_{ts} B^t P B (B^t P B C_{ss} B^t P B + \sigma_n^2 B^t P B)^{-1} B^t P B C_{st} \quad (A.17)$$

Moreover, indicating with the symbol e the error in the estimate of the predicted signal, i.e. the difference between its theoretic and its estimated value: $e = t - \hat{t}$, by applying the law of variance propagation, and taking into account expression (A.17), the covariance matrix C_{ee} becomes:

$$C_{ee} = C_{tt} - C_{\hat{t}\hat{t}} = \qquad (A.18)$$

$$= C_{tt} - C_{ts} B^t PB \, (B^t PBC_{ss} B^t PB + \sigma_n^2 \, B^t PB)^{-1} B^t PBC_{st}$$

Unfortunately, expressions (A.17) and (A.18) are not very convenient in computation, and it is not possible to find others more suitable. Therefore their computation is usually omitted.

Some statistic properties of the mentioned estimates are now considered. The estimate for the filtered and predicted signal is consistent and unbiased under the hypothesis that the expected value of the observables is zero. The estimate of the filtered and predicted signal and the estimate of its error are efficient, i.e. their variance is smaller than the a priori variance of the signal. The estimate for the residual noise is efficient, i.e. its variance is smaller than the a priori variance of the observations. The estimate of the filtered and predicted signal has minimal variance of all linear estimates.
The variance of the noise can also be estimated a posteriori. Imposing its estimate to be unbiased,

$$k\sigma_n^2 = k \, E(\hat{\sigma}_n^2) = E(\hat{n}^t P \hat{n}) = Tr(PC_{\hat{n}\hat{n}}) \qquad (A.19)$$

one obtains:

$$k = m - n + Tr[\sigma_n^2 \, P^{1/2} B \, (B^t PBC_{ss} B^t PB +$$

$$+ \sigma_n^2 \, B^t PB)^{-1} B^t P^{1/2}] \qquad (A.20)$$

where m is the number of observations and n the number of parameters. Therefore the a posteriori estimate of the variance of the noise becomes:

$$\hat{\sigma}_n^2 = (\hat{n}^t P \hat{n})/k \qquad (A.21)$$

This estimate is also consistent under the hypothesis that the observations are normally distributed. Formula (A.19) can be used for the a posteriori estimate of variances and therefore also of weights of a priori defined groups of observations.
The a posteriori estimate of the covariance function of the signal requires fairly sophisticated procedures, which are often computationally heavy and do not always produce reliable results.
With respect to the computability some considerations are made concerning the applications of theorems (A.4) and (A.5). As was already said before, a suitable application of these theorems provides systems of dimension n <m, without inverse matrices which contain other inverse matrices. The expressions (A.7) and (A.12) contain the expressions:

$$(B^t PB)^{-1} BP\alpha^\circ \quad ; \quad (B^t PB)^{-1} \qquad (A.22)$$

The solution of this system and the computation of the inverse matrix are standard procedures in any least squares problem and, are computable with direct solution algorithms, which are capable to work with sparse matrices. Expressions (A.7) and (1.12) also contain the expressions:

$$(B^t PBC_{ss} B^t PB + \sigma_n^2 \, B^t PB)^{-1} B^t P\alpha^\circ$$

$$(B^t PBC_{ss} B^t PB + \sigma_n^2 \, B^t PB)^{-1} \qquad (A.23)$$

The normal matrix $B^t PB$ was already obtained before. The covariance matrix: $C_{ss} = C^\circ_{ss} * S_{ss}$, of the properly called stochastic parameters is a sparse matrix when constructed by multiplying, according to Hadamard, the proper covariance matrix C°_{ss} by a suitable finite covariance matrix S_{ss}. Its sparseness depends on the "persistence of correlation" of the finite covariance functions. Its dispersion however is influenced by the (re)numbering of the points. The product of three sparse matrices $(B^t PB)C^t_{ss}(B\,PB)$ is a sparse matrix itself. The solution of the corresponding system therefore can be computed with iterative solution algorithms for sparse matrices.
Finally starting from the use of the Hadamard product to obtain a sparse covariance matrix, an acceptable approximation of its inverse matrix can be obtained by multiplying, according to Hadamard, once more the inverse of the covariance matrix $(C^\circ_{ss} * S_{ss})^{-1}$ by the previous defined finite covariance matrix S_{ss}. In such a way the matrix $(C^\circ_{ss} * S_{ss}) * S^{-1}_{ss}$ is sparse too and the expressions:

$$(\sigma_n^2 \, (C^\circ_{ss} * S_{ss})^{-1} * S_{ss} + B^t PB)^{-1} \, B^t P \, \alpha^\circ$$

$$(\sigma_n^2 \, (C^\circ_{ss} * S_{ss})^{-1} * S_{ss} + B^t PB)^{-1} \qquad (A.24)$$

could be preferred to the expressions (A.23) in term of a greater sparseness of the matrices and a better numerical conditioning of the systems. This new approach, which could be called "approximated integrated geodesy", has not been tested very well yet, but should be applied in the next future.

REFERENCES

Ammannati, F., Benciolini, B., Mussio, L., Sansò, F. (1983). An Experiment of Collocation Applied to Digital Height Model Analysis. Proceedings of the Int. Colloquium on Mathematical Aspects of Digital Elevation Models, K. Torlegard (Ed), Dept. of Photogrammetry, Royal Institute of Technology, Stockholm, 19-20 April, 1983.

Barzaghi, R., Crippa, B., Forlani, G., Mussio, L. (1988). Digital Modelling by Using the Integrated Geodesy Approach. Int. Archives of Photogrammetry and Remote Sensing, vol. 27, part B3, Kyoto, 1-10 July, 1988.

Barzaghi, R., Crippa, B., (1990). 3-D Collocation Filtering. Int. Archives of Photogrammetry and Remote Sensing, vol. 28, part 5/2, Zurich, 3-7 September, 1990.

Crippa, B., Mussio, L., (1987). The New ITM System of the Programs MODEL for Digital Modelling. Proceedings of the Int. Colloquium on Progress in Terrain Modelling, O. Jacoby and P. Frederiksen (Eds), Technical University of Denmark, Copenhagen, 20-22 May, 1987.

Crippa, B., De Haan, A., Mussio, L., (1989). The Formal Structure of Geodetic and Photogrammetric Observations. Proceedings of the ISPRS IC-WG III/VI Tutorial on "Mathematical Aspects of Data Analysis", Pisa, 1-2 June, 1989.

Dahm, W., Southerland, K., Buch, K. (1990). Four-dimensional Laser Induced Flourescence Measurements of Conserved Scalar Mixing in Turbulent Flows. Proocedings 5th Int. Symposium on the Application of Laser Techniques in Fluid Mechanics, Lisbon, 9-12 July, 1990.

De Haan, A., Mussio, L., (1989). Kinematic Levelling Adjustments with Polynomials and Polynomial Splines. Geodesia e Scienze Affini, n. 3, 1989.

Maas, H.G., (1990). Digital Photogrammetry for Determination of Tracer Particle Coordinates in Turbulent Flow Research. Int. Archives of Photogrammetry and Remote Sensing, vol. 28, part 5/1, Zurich, 3-7 September, 1990.

Maas, H.G., (1992a). Digitale Photogrammetrie in der Dreidimensionalen Stromungsmesstechnik. Ph. D. Thesis No. 9665, ETH Zurich.

Maas, H.G., (1992b). Complexity Analysis for the Establishment of Image Correspondences of Dense Spatial Target Fields. Int. Archives of Photogrammetry and Remote Sensing, vol. 29, in printing.

Malik, N., Dracos, T., Papantoniou, D., Maas, H.G., (1992). Particle Tracking Velocimetry in Three-dimensional Turbulent Flows - Part II: Particle Tracking and Langrangian Trajectories, Short Course on Flow Visualization and Flow Structures, Zurich, 30 March - 3 April, 1992.

Papantoniou, D., Dracos, T., (1989). Analyzing 3D Turbulent Motion in Open Channel Flow by Use of Stereoscopy and Particle Tracking. Advances in Turbulent 2, H.H. Hernholz and H.E. Fiedler (Eds), Springer-Verlag.

Papantoniou, D., Maas, H.G., (1990). Recent Advances in 3D Particle Tracking Velocimetry. Proceedings 5th International Symposium on the Application of Laser Techniques in Fluid Mechanics, Lisbon, 9-12 July, 1990.

Sansò, F., Tscherning, C.C. (1982). Mixed Collocation: a Proposal.Quaternones Geodaesiae, University of Thessaloniki, 3 January, 1982.

Sansò, F., Schuh, W.D. (1987). Finite Covariance Functions. Bulletin Geodésiqué, n. 61, 1987.